Thi Yen Nguyen, Ernst A. Roessler, Klaus Rademann and Franziska Emmerling*

Control of organic polymorph formation: crystallization pathways in acoustically levitated droplets

DOI 10.1515/zkri-2016-1964
Received May 31, 2016; accepted July 18, 2016; published online August 22, 2016

Abstract: Theoretical and experimental studies indicate that crystal nucleation can take more complex pathways than expected on the ground of the classical nucleation theory. Among these pathways are the formation of pre-nucleation clusters and amorphous precursor phases. A direct *in situ* observation of the different pathways of nucleation from solution is challenging since the paths can be influenced by heterogeneous nucleation sites, such as container walls. Here, we provide insights into the crystallization process using the *in situ* combination of an acoustic levitator, Raman spectroscopy, and X-ray scattering. The contactless sample holder enables the observation of homogeneous crystallization processes and the detection of intermediates and final crystalline forms. We provide evidence for the existence of multiple pathways of nucleation based on the investigation of the crystallization of organic molecules from different solvents. Starting from a diluted solution, a supersaturation is reached during the experiment due to the evaporation of the solvent. The highly supersaturated solution reveals different pathways of crystallization. Depending on the degree of supersaturation either the thermodynamically stable or the metastable crystal form is observed.

Keywords: crystallization; *in situ* XRD; polyamorphism; polymorphism; raman spectroscopy.

***Corresponding author: Franziska Emmerling,** BAM Federal Institute for Materials Research and Testing, Richard-Willstaetter-Strasse 11, 12489 Berlin, Germany,
E-mail: franziska.emmerling@bam.de
Thi Yen Nguyen: BAM Federal Institute for Materials Research and Testing, Richard-Willstaetter-Strasse 11, 12489 Berlin, Germany
Ernst A. Roessler: Institute of Physics, Universitaet Bayreuth, Bayreuth 95440, Germany
Klaus Rademann: Department of Chemistry, Humboldt Universitaet zu Berlin, Brook-Taylor-Strasse 2, 12489 Berlin, Germany

Introduction

Nucleation is the first step towards crystallization. Atoms, ions, and particles aggregate to form crystal nuclei. According to the classical nucleation theory (CNT), nucleation is governed by two counteracting energies i) the interfacial free energy and ii) the volume Gibbs free energy between liquid and crystal phases. The interfacial free energy prevents the formation of the nuclei working as an energy barrier, while the volume Gibbs free energy eventually stabilizes the crystal nuclei. A high crystal-liquid interfacial free energy leads to a high energy barrier which hampers crystallization, allowing the liquid to supercool or supersaturate. The crystal-liquid interfacial energy arises from configurational entropy differences between crystal and liquid phases. Pronounced differences in the local structural ordering between the crystal phase and the liquid phase lead to an increased interfacial energy and consequently to a higher nucleation barrier [1, 2]. Experimental and theoretical studies indicated that the CNT might not be adequate for the description of the initial nucleation process [3–13]. The so-called multi-pathway nucleation mechanism was introduced recently for supersaturated solutions [3, 7, 9–13]. Within this mechanism, nucleation does not proceed directly from solution, but includes intermediate stages i.e. the formation of pre-nucleation clusters, amorphous states, or a dense liquid. This two-step nucleation process has been observed for several systems [3, 4, 6]. *In situ* methods are mandatory to study the processes occurring during the early stages of the formation of crystalline solids [14]. It is of interest, whether the same nucleation process can be observed in highly supersaturated systems as under low supersaturation. To investigate the difference, a scenario must be provided where a high level of supersaturation is achieved. To access these levels of supersaturation any container walls which might act as heterogeneous nucleation sites have to be circumvented. In the past few years, acoustic levitators generating an ultrasonic standing wave for the containerless levitation of objects, such as droplets or solid samples, have gained considerable

interest to study crystallization processes [15–26]. We briefly describe the experimental development up to the introduction of a climate unit for the control of the chemical potential of the surrounding vapor phase [27]. First experiments using an acoustic levitator in combination with X-ray analysis consisted of a sample preparation step and *ex situ* diffraction experiments. Nagashio et al. investigated the containerless processing of the superconducting oxide $NdBa_2Cu_3O_{7-d}$(Nd123) by combining acoustic levitation with CO_2 laser heating [28]. The specimens obtained were then characterized in *ex situ* X-ray diffraction (XRD) experiments. Preliminary test regarding the feasibility of the acoustic levitation in combination with *in situ* synchrotron X-ray diffraction were carried out by Cerenius et al. [29]. Our group pioneered a few years ago with the first time resolved *in situ* XRD experiments providing a continuous set of XRD patterns during a crystallization process [17, 18, 30]. In one of the early experiments, the non-classical crystallization pathway of calcium carbonate system involving a liquid/liquid phase separation and an emulsified of a highly hydrated liquid amorphous calcium carbonate (LACC) was investigated [20, 31]. The LACC develops from pure, neutral, and saturated calcium bicarbonate solution crystallizing homogeneously in acoustic levitation [20]. These characteristic intermediates behave like a classical emulsion and are stabilized electrostatically [31]. Extended studies with additives resulted in destabilization phenomenon of LACC precursor using lysozyme, whereas the glycoprotein ovalbumin stabilizes this transient state, which carries a negative surface charge, and prevents undirected mineralization of the eggshell [32]. The crystallization processes of organic compounds were investigated by performing *in situ* XRD and in a further development Raman spectroscopy combined with XRD experiments. This experimental setup is capable of providing comprehensive and simultaneous information from these complementary analytical methods in a single experiment. A prerequisite for XRD is the existence of a crystalline solid consisting of several unit cells, typically more than ten per edge. In order to investigate the structure of transient crystalline or amorphous intermediates Raman spectroscopy enables *in situ* monitoring of the solution, amorphous forms, crystal formation, and transformation from one polymorph to another one. The custom-made acoustic levitator including a climatic unit allows the control of the sample surrounding regarding the humidity and temperature [27].

We examine the crystallization process of the organic materials ROY (5-methyl-2-[(2-nitrophenyl)amino]-3-thiophenecarbonitrile), nifedipine, and paracetamol which have high tendency to form different crystal structures. The highly reproducible studies under controlled humidity and temperature using combined XRD and Raman spectroscopy indicate a strong dependence of the crystallization pathways on the solvent used for the crystallization and the surface. By using a contactless sample holder, solid surfaces are eliminated which enables the homogeneous crystallization. The choice of the solvent can push the crystallization progress to form a favored crystal structure of an organic molecule. This advantage is used to isolate pure crystal phases of the samples. For paracetamol we found experimental evidence that depending on the solvent different amorphous forms are preferred (polyamorphism) leading to the crystallization of a distinct polymorph. Further *in situ* scattering crystallization experiments with the main focus on the influence of the concentration on the crystallization pathway show that crystallization starting from low concentrated solutions (S = 0.1) forms crystal structures which differ from the highly saturated ones ($S \approx c_s$). Different pathways of crystallization exist and they are triggered by the saturation of the solutions.

Experimental setup

Acoustic levitation

The custom-made levitator used for our experiments consists of three main components: the sonotrode, the reflector, and an atmosphere controlling device (see Figure 1A). The ultrasonic field is emitted by the sonotrode and it is generated by a piezoelectric crystal working with an oscillating frequency of 58 kHz. A standing wave with several sound pressure nodes between the sonotrode and the concentric reflector emerges by adjusting the distance of a multiple of half the used wavelength. Axial radiation pressure and radial Bernoulli stress forces hold liquids and solid samples in a fixed, levitated and contactless position. Levitated samples can reach a volume of up to 12 µL with the corresponding diameter of around 2.8 mm and a mass of 12 mg. Further sample requirements, such as magnetic or dielectric properties are not needed. A custom-made device allows controlling the humidity and temperature at the sample position by introducing a heatable/coolable nitrogen gas flow which is saturated with water or heated up with the heating device.

Application and analytical methods

The acoustic levitator is used in combination with two analytical methods, time-resolved X-ray scattering and Raman spectroscopy. The *in situ* X-ray diffraction experiments were performed at the µSpot beamline (BESSY II, Helmholtz Center Berlin for Materials and Energy). The experiments were typically performed with a beam diameter of 100 µm at a photon flux of 1×10^9 s^{-1} at a ring current of 100 mA. The experiments were performed with a wavelength of 1.0 Å

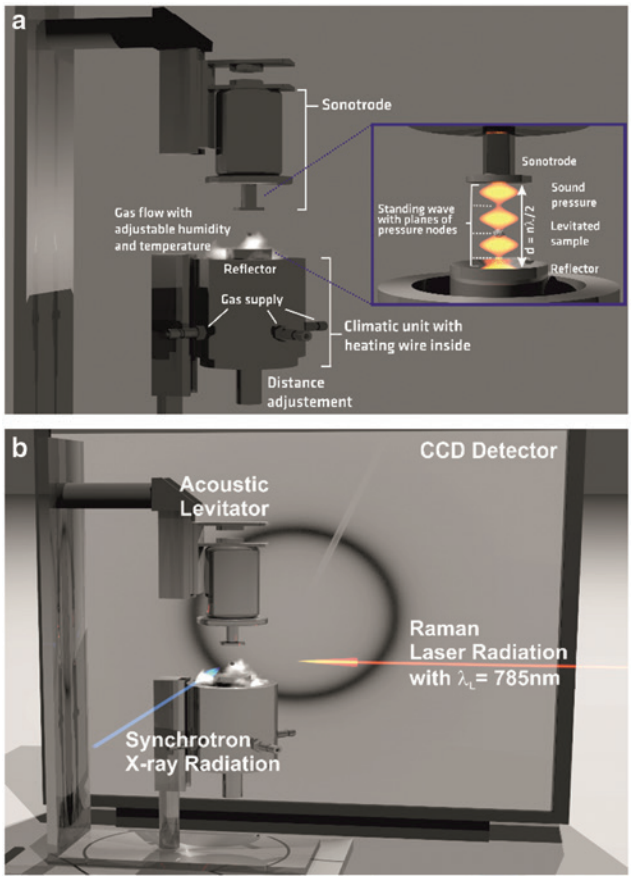

Fig. 1: (a) Schematic overview of the acoustic levitator and its operating principle. (b) Setup for crystallization studies with the acoustic levitator and combined *in situ* synchrotron XRD and Raman spectroscopy. A 2D CCD detector is used to record the X-ray scattering signal. The droplet size is monitored throughout the experiment with a CCD camera. In a typical experiment a solution with different initial concentrations of a given analyte is levitated. As the solvent evaporates, the concentration reaches supersaturation and a following fast crystallization step occurs.

using a double crystal monochromator (Si 111). Scattered intensities were collected with a two-dimensional X-ray detector (MarMosaic, CCD 3072 × 3072) and time resolution of 15 s [33]. The obtained scattering images were processed employing an algorithm from the computer program FIT2D [34]. The Raman measurements were performed with a Raman RXN1™ Analyzer (Kaiser Optical Systems, Inc., Ecully, France) using NIR excitation at 785 nm and an irradiance of 6.4 W/cm^2 on the sample. An acquisition time of 5 × 5 s or 8 × 1 s was chosen resulting in a time resolution of 30 s or 15 s, respectively. The acquisition of XRD and Raman data simultaneously within an approx. 20 s period permits the determination of phase composition from the onset of the first molecular assemblies to the final crystalline structure. The volume of the shrinking droplet is monitored through the experiments based on the shadowgraph of the droplet. By using a reference object with known size, the volume and concentration of the droplet is available. The humidity (R_H = 17.5 ± 2.5%) and temperature (T = 22.0 ± 1.0 °C) maintain constant during all crystallization experiments.

Materials

5-Methyl-2-[(2-nitrophenyl)amino]-3-thiophenecarbonitrile (ROY, ≥98%) was purchased from Intatrade Chemicals GmbH (Muldestausee, Germany) and purified by recrystallization from absolute ethanol (Merck KGaA, Darmstadt, Germany). The product consisted mainly of yellow crystals and small amounts of orange and red crystals. After separation from the supernatant solution, the crystals were dried, manually sorted, and characterized by X-ray diffraction (Bruker AXS, D8, Cu $K_{\alpha 1}$ radiation) and Raman spectroscopy. The yellow crystals were identified as the Y modification of ROY ($P2_1/n$, a = 8.5001(8) Å, b = 16.413(2) Å, c = 8.5371(5) Å, β = 91.767(7)°, V = 1190.46 Å^3). The small portions of orange and red crystals were determined as polymorphs ON and R, respectively. Other contributions were not detectable. Solutions of ROY were prepared from the sorted crystals in organic solvents.

Nifedipine (≥98%) was purchased from Sigma-Aldrich (CAS 21829-25-4) and used without further purification. The X-ray diffraction pattern (Bruker AXS, D5000, Cu $K_{\alpha 1}$ radiation) revealed that the sample consisted of the α-modification ($P2_1/c$, a = 10.923(5) Å, b = 10.326(6) Å, c = 14.814(7) Å, β = 92.70(6)°, V = 1669.03 Å^3).

Paracetamol (≥99% purity, Sigma-Aldrich) was used without purification. Based on powder X-ray diffraction (Bruker AXS, D8 Discover, Cu $K_{\alpha 1}$ radiation) and Raman spectroscopy the compound was identified as the thermodynamically stable monoclinic form I. Paracetamol was dissolved in different organic solvents with concentrations half the corresponding saturation. In methanol, different concentrations referring to the saturation (S = 0.1, 0.8, 1) were prepared.

Acetone (≥99.5%) was purchased from Th. Geyer GmbH & Co. KG (Renningen, Germany), acetonitrile (≥99.8%) from J. T. Baker (Deventer, The Netherlands), benzonitrile (99%) from Acros Organics (Geel, Belgium), dichloromethane (≥99.5%) and methanol (≥99.9%) from Carl Roth GmbH + Co. KG (Karlsruhe, Germany), ethyl acetate (≥99.5%) from Fluka Chemie GmbH (Buchs, Switzerland), and 1-propanol (≥99.5%) from MerckKGaA (Darmstadt, Germany).

Results

The crystallization processes of the compounds given in Table 1 were studied in detail using an acoustic levitator in combination with *in situ* X-ray scattering and Raman spectroscopy.

ROY (5-methyl-2-[(2-nitrophenyl)amino]-3-thiophenecarbonitrile is a highly polymorphic compound with ten known crystalline structures [35, 36]. The short name stems from the red, orange and yellow color of the crystals which arise from the various molecular conformations in the different crystalline modifications [44]. The crystallization and the influence of the pure solvent on the selective isolation of ROY polymorphs from solution were investigated [26]. By controlling temperature, humidity, and the surface the influence of the solvent is the determining factor in the crystallization pathway. The acquisition of XRD and Raman data simultaneously within a 20 s period

Tab. 1: Overview of the studied compounds.

Compound	Structure	Polymorphs
ROY (5-methyl-2-[(2-nitrophenyl)amino]-3-thiophenecarbonitrile	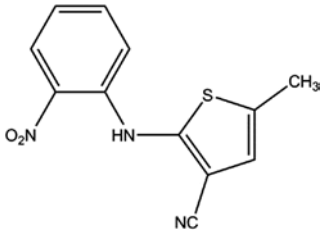	Y (yellow prism) [35] ON (orange needles) [35] R (red prism) [35] YN (yellow needles) [36] OP (orange plate) [36] ORP (orange) [36] YT04 (yellow prism) [36] Y04 (yellow) [36] RPL (red plate) [37] R05 (red) [36]
Nifedipine	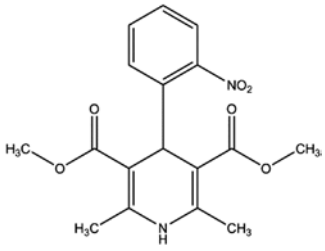	α [38] β [39] γ [40]
Paracetamol	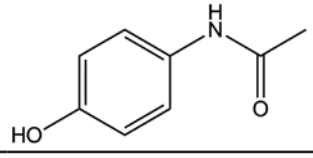	Form I [41] Form II [42] Form III [43]

permits the determination of phase composition from the onset of the first molecular assemblies to the final crystalline structure (see Figure 2). The crystallization was monitored using different solvents [acetone, acetonitrile (ACN), benzonitrile, dichloromethane (DCM), ethyl acetate (EtOAc), methanol (MeOH), 1-propanol]. The coupled methods *in situ* XRD and Raman spectroscopy provide an unambiguous identification of the different ROY forms. In Figure 2 the crystallization of ROY from a solution in methanol is shown exemplarily. Under these conditions the metastable form YN is obtained as a pure phase. An amorphous phase is built during the process of solvent evaporation in a time span of 8 min. The pure amorphous phase is stable for about 10 min. Subsequently, the final product YN crystallizes within 3 min from the amorphous form. The crystallization process takes around 20 min.

The schematic summary of the crystallization shows the progress from different organic solvents (see Figure 3).

Four polymorphs could be identified as final and solely formed crystallization products. Form Y is the thermodynamically stable polymorph of the known forms and YN is the least stable one regarding the free energy. The R form is the second least stable modification. ON is more stable than YN and R, and enantiotropically related to Y. For all solvents except for ACN, a concentration-dependent formation of polymorphs occurs. In all cases, the crystallization of a pure modification was observed. Crystallization of form Y seems to be favored in presence of solvent, whereas the polymorphs R, YN and ON develop from an amorphous precursor. In solution the nitrophenyl and the thiophene rings of ROY molecules are arranged perpendicularly. The forms Y and YN adopt a similar alignment which is supposed to be reason for the promoted formation of stable Y with solvent molecules. Another aspect is the nucleus formation requesting specific arrangement of molecules which can be exacerbated by remaining solvent molecules. Thus, the distances of the centers of gravity of the molecules have to be considered. The polymorphs show distinctive differences in their nearest environment. In form YN and ON the nearest neighbors are much closer in comparison to Y and R. Solvent molecules can hamper the arrangement of the ROY molecules. The influence of the solvent on the crystallizing form was also evaluated using Hansen solubility parameters. They describe the ability of a compound for molecular interactions of nonionic liquids by a dispersion force component δ_D, a hydrogen bonding force component δ_H, and a polar force component δ_P. The ROY molecules

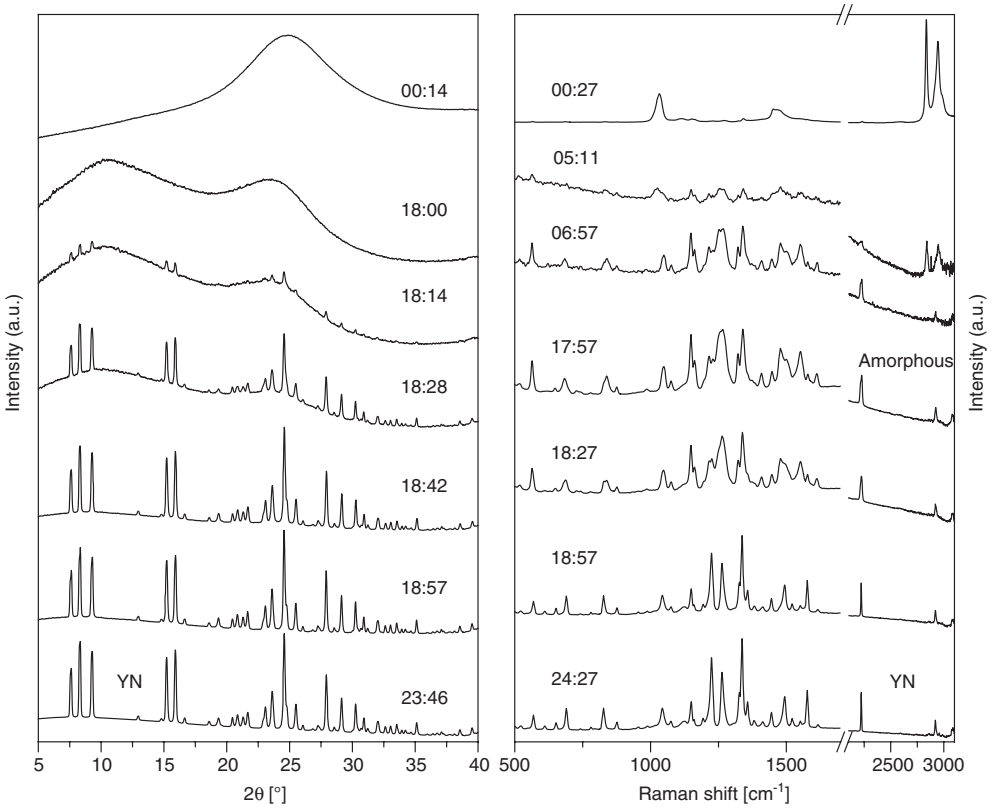

Fig. 2: *In situ* X-ray diffraction pattern (left) and Raman spectra (right) recorded during the crystallization of ROY from a solution in methanol using an acoustic levitator as a sample holder. The evaporation of the solvent leads to the formation of an amorphous phase which crystallizes to the YN polymorph.

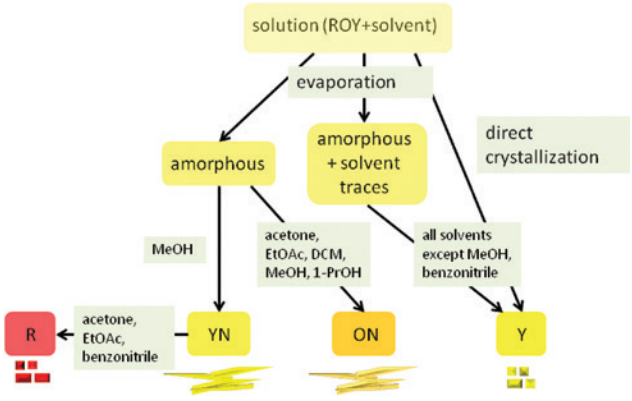

Fig. 3: Schematic summary of the crystallization pathways of ROY from different solvents.

in Y and YN adopt nearly the same conformation. Thus these two forms are favored in solvents which show either hydrogen bonding ability (MeOH) or high polarity (ACN). YN is formed from MeOH as the final product and from acetone, EtOAc, and benzonitrile as an intermediate prior the crystallization of R. The characteristic crystallization indicates the influence of the solvent on the amorphous precursor. The results suggest that the crystallization of a specific polymorph can be attributed to nearest neighbor interactions and intermolecular attractive forces between solvent and analyte.

Using the tandem approach with acoustic levitation we succeeded also in elucidating the crystallization process of the pharmaceutical nifedipine from different organic solvents. Different crystallization routes were discovered depending on the solvent (Dichlormethane (DCM), ACN, MeOH, acetone, EtOH) [45]. Nifedipine has three known crystalline modification: α, β, and γ [38–40]. The crystallization process follows different pathways including the crystalline structures (see Figure 4). Whenever the formation of hydrogen bonds between solvent (acetone, ethanol) and solute is possible, the crystallization of the

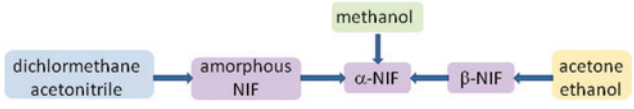

Fig. 4: Schematic overview of the transformation behavior of nifedipine from different solvents during homogeneous crystallization in an acoustic levitator.

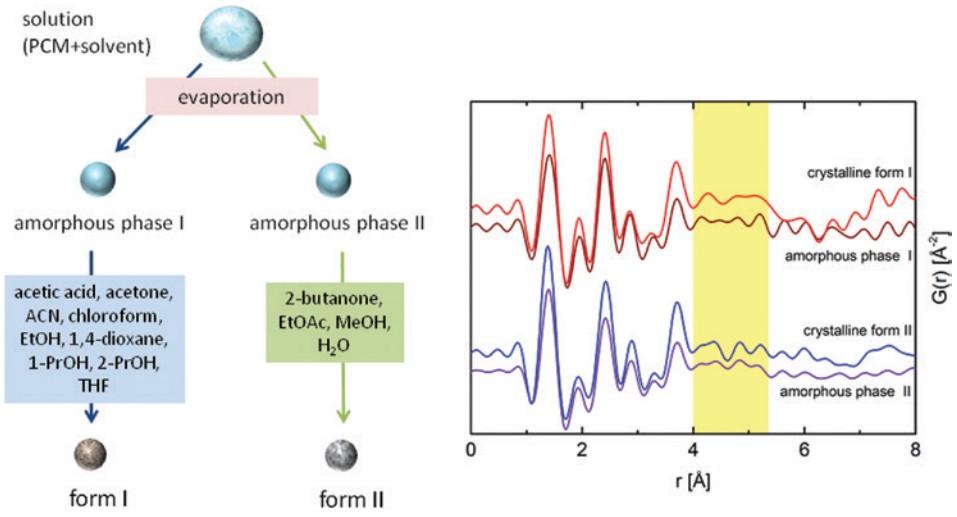

Fig. 5: Summary of the crystallization of paracetamol from solution in different solvents via amorphous precursors to the crystalline form I or selectively form II (left). The respective pair distribution function (PDF) analysis of the amorphous phases and the crystalline products revealed the relation of the amorphous precursor to the specific crystalline form (right).

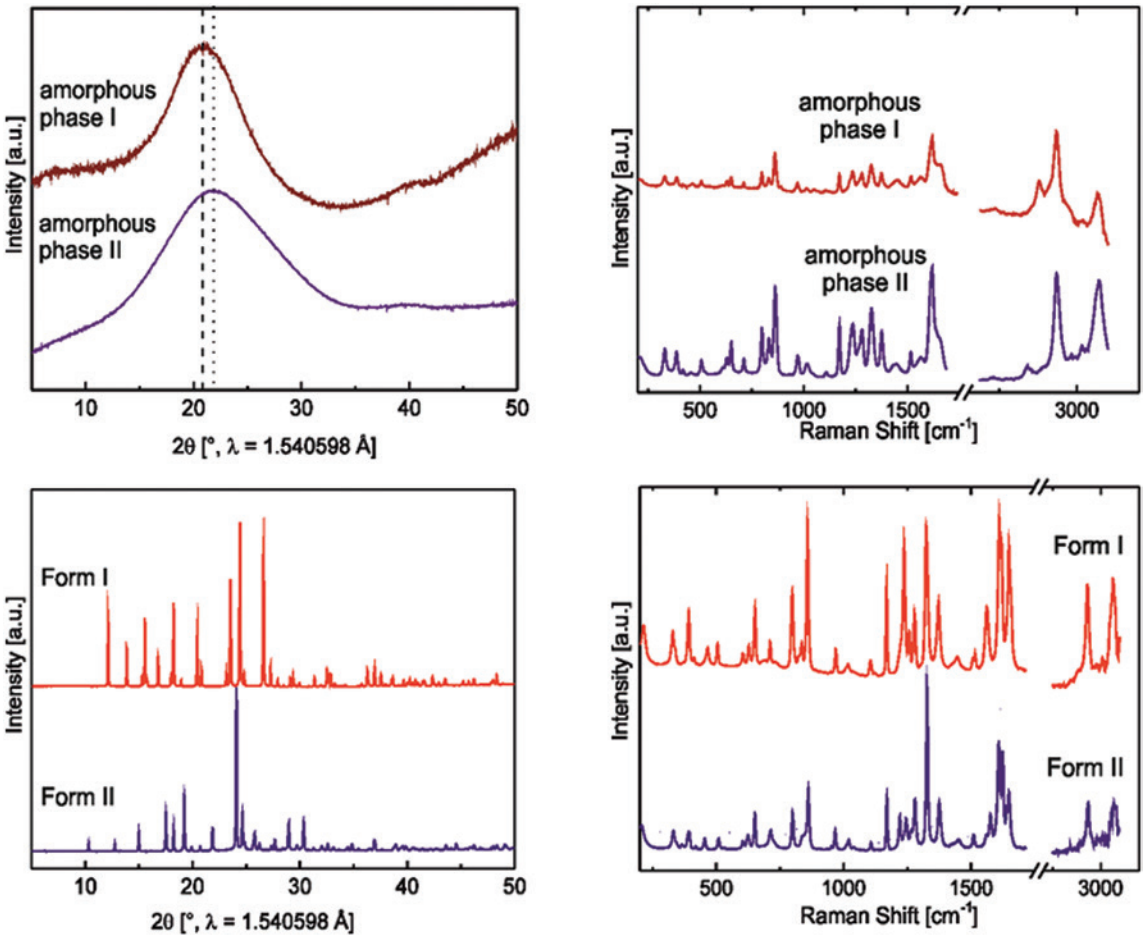

Fig. 6: XRD and Raman spectra of the amorphous precursors (top) and the crystalline form I and form II (bottom). The different amorphous forms can be identified by a shift of the maximum of the amorphous halo and from the respective Raman spectra.

thermodynamically stable α-polymorph proceeds via the intermediate β-form of nifedipine. Without such interactions, e.g. in case of DCM and ACN, the glassy modification is formed intermediately prior to the crystallization of α-form. These observations are consistent with Ostwald's rule of stages [46, 47].

All crystallization studies of pharmaceuticals from solution so far showed a strong correlation between crystallization pathways, polymorphic structures, the used solvents and the presence of surface. For the experiments with paracetamol additional information from pair distribution function (PDF) analysis provided direct evidence of the phenomenon polyamorphism [48] of an organic compound [25]. The ability to have more than one amorphous state is known for inorganic materials [49, 50]. The crystallization of paracetamol was investigated using *in situ* XRD with PDF and Raman spectroscopy. Depending on the solvent different crystallization pathways were observed leading to the thermodynamically stable form I or the metastable form II (see Figure 5 left; see Figure 6 bottom). The disordered nature of amorphous precursors gives rise to diffuse scattering, which contains valuable information on interactions and can give insights into short and medium range ordering. The pair distribution function, G(r), is essentially a map of atom–atom distances and can be used to ascertain the degree of local and intermediate ordering within amorphous solids. In the case of paracetamol, both crystallization pathways proceed through the corresponding amorphous intermediates (amorphous phase I and II).

The XRD and Raman spectra of these intermediate states are shown in Figure 6 (top) The intrinsic structures of the amorphous precursors are directly related to the final structures of the polymorphs (see Figure 5, right). The PDF analysis indicates a similar atom distance distribution probability until 6 Å between the amorphous state and the resulting crystalline form. The amorphous phases represent precursors with pre-orientation of the analyte molecules introduced by the corresponding solvent. This example illustrates that solvents can also influence the formation of a characteristic amorphous precursor which determines the outcome of the final crystallization product.

In a further experiment, we investigated the influence of the saturation level on the crystallization of paracetamol. Different initial concentrations of paracetamol in methanol were chosen and the crystallization process was investigated under reproducible conditions at a temperature of T = 22.0 ± 1.0 °C and a relative humidity of R_H = 17.5 ± 2.5%. On the basis of the shadow images, the evaporation time of the solvent was quantified by observing the shrinking droplets (see Figure 7A).

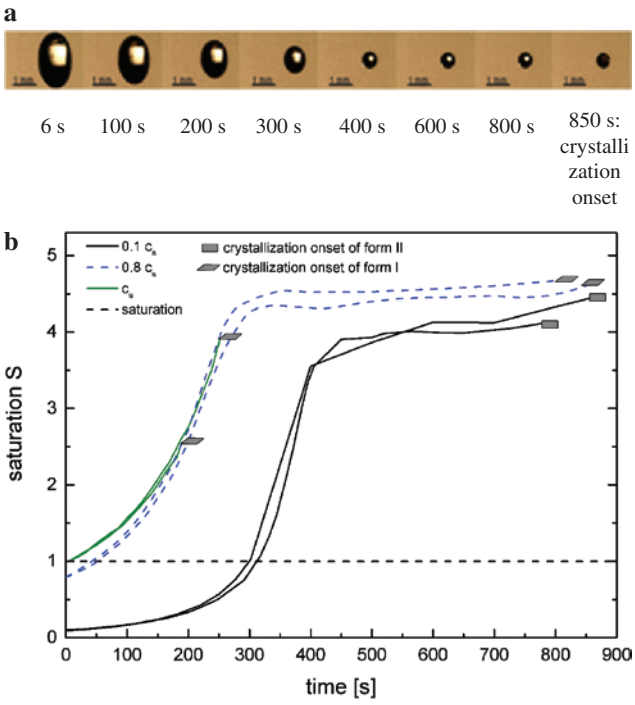

Fig. 7: (a) Continuous decrease of the droplets' size (methanolic paracetamol solution) and the transition from the liquid to the solid phase during a levitation time of 850 s. Droplet is shrinking in diameter from 2.0 to 0.6 mm. (b) Saturation ratio ($S=c/c_s$; c_s=1.45 mol/L) as a function of time during the crystallization experiment. Starting from paracetamol solutions with different initial concentrations (see color code) with respect to the saturation concentration of paracetamol the process was followed with *in situ* XRD until the onset of crystal growth is observed (parallelogram: crystallization of form I, rectangle: crystallization of form II). Different lines with the same color stem from repeated experiments.

Under the described conditions, the droplet shrinks significantly within a few minutes leading to a fast increase of the supersaturation ratio of the solution. From methanol, the formation of form II was always observed in previous experiments starting from diluted solutions below the saturation concentration (S = 0.1). For solutions with a starting saturation level of S = 1, a direct crystallization of form I is observed (green lines, Figure 7B). Crystallization experiments starting with a concentration below supersaturation (S = 0.8) show also a fast evaporation of methanol in the range of 200–250 s after initiation of the experiment, followed by a prolonged period in which an amorphous precursor is observed (blue dashed lines, Figure 7B). Finally, form I crystallizes from the amorphous precursor. For solutions well below supersaturation (S = 0.1) a slower evaporation is observed, which is finished after 300–400 s. Subsequently, an amorphous phase persists starting from 400 s and crystallizes finally to form II (black lines, Figure 7B). The experiments show, that for a

given solvent, the variation of the concentration can also affect the crystallization pathway. Whether an amorphous phase is formed or not is determined by the number of solvent molecules. For the saturated solutions (S = 1) no amorphous intermediates were observed. For solutions with concentrations below saturation, the formation of an amorphous form was always observed. Considering that different polymorphs crystallize from these amorphous precursors and the known polyamorphism of paracetamol, we can speculate that not only the nature, but also the number of present solvent molecules in a supersaturated solution triggers the formation of the crystallizing polymorph. This highly interesting phenomenon is an aspect of our current research.

Conclusion

Crystallization from solutions follows specific pathways different from those predicted by the CNT. To study these pathways it is of utmost importance to eliminate any possible influencing factors, so that the system is stabilized in an undisturbed levitated environment. Under acoustic levitation it is possible to study homogeneous crystallization processes using different analytical techniques. The *in situ* combination of XRD and Raman spectroscopy proves to be a powerful technique for the screening of crystallization from solution. Raman spectroscopy is suitable for the characterization of solutions, amorphous intermediates and crystalline stages. Both methods provide a deeper insight into early stages of crystallite forming processes during the evaporation of solvents. The application of pair distribution function (PDF) analysis from XRD data indicates the presence of polyamorphism in paracetamol. The different amorphous states are crucial intermediates whose properties are determined by the used solvents. The choice of the solvent and the degree of supersaturation triggers and controls certain crystallization pathways and allows obtaining a desired crystalline modification.

The most salient results are the following:

(i) The phenomenon of polyamorphism has been observed for the first time for paracetamol during the crystallization process referring to a broad selection of solvents.

(ii) The formation of the two different amorphous phases, phase I and phase II, is engendered by the individual nature of the solvent. This is true for half saturated solutions. A systematic classification has not been completed by now. More experiments and theoretical studies are needed.

(iii) Another unexpected observation is the fact that the initial concentration of the methanolic paracetamol solution is crucial for the final crystalline polymorphic forms, I or II. Practical experiences have shown that higher initial concentrations near the saturation c_s yield selectively form I. For S = 1 crystallization starts directly from solution. An amorphous intermediate phase seems to be avoided under these conditions. By way of contrast, very low initial concentrations around S = 0.1 provide eventually form II out of an amorphous precursor phase.

We anticipate that our results open new venues for studying multiple pathways for crystallization in solution systems.

Acknowledgements: We gratefully acknowledge financial support by the Deutsche Forschungsgesellschaft through SPP 15415 (crystalline non-equilibrium phases and polymorphs): Ra494/15-1, Ro907/14-1 and Em198/4-1.

References

[1] K. F. Kelton, G. W. Lee, A. K. Gangopadhyay, R. W. Hyers, T. J. Rathz, J. R. Rogers, M. B. Robinson, D. S. Robinson, First X-ray scattering studies on electrostatically levitated metallic liquids: demonstrated influence of local icosahedral order on the nucleation barrier. *Phys. Rev. Lett.* **2003**, *90*, article no: 195504.

[2] C. G. Tang, P. Harrowell, Anomalously slow crystal growth of the glass-forming alloy CuZr. *Nat. Mater.* **2013**, *12*, 507.

[3] P. R. tenWolde, D. Frenkel, Enhancement of protein crystal nucleation by critical density fluctuations. *Science* **1997**, *277*, 1975.

[4] P. G. Vekilov, Dense liquid precursor for the nucleation of ordered solid phases from solution. *Cryst. Growth Des.* **2004**, *4*, 671.

[5] D. Kashchiev, P. G. Vekilov, A. B. Kolomeisky, Kinetics of two-step nucleation of crystals. *J. Chem. Phys.* **2005**, *122*, article no: 244706.

[6] D. Gebauer, A. Volkel, H. Colfen, Stable prenucleation calcium carbonate clusters. *Science* **2008**, *322*, 1819.

[7] D. Erdemir, A. Y. Lee, A. S. Myerson, Nucleation of crystals from solution: classical and two-step models. *Accounts Chem. Res.* **2009**, *42*, 621.

[8] P. G. Vekilov, Nucleation. *Cryst. Growth Des.* **2010**, *10*, 5007.

[9] P. G. Vekilov, The two-step mechanism of nucleation of crystals in solution. *Nanoscale* **2010**, *2*, 2346.

[10] Q. Hu, M. H. Nielsen, C. L. Freeman, L. M. Hamm, J. Tao, J. R. I. Lee, T. Y. J. Han, U. Becker, J. H. Harding, P. M. Dove, J. J. De Yoreo, The thermodynamics of calcite nucleation at organic interfaces: classical vs. non-classical pathways. *Faraday Discuss.* **2012**, *159*, 509.

[11] A. F. Wallace, L. O. Hedges, A. Fernandez-Martinez, P. Raiteri, J. D. Gale, G. A. Waychunas, S. Whitelam, J. F. Banfield,

J. J. De Yoreo, Microscopic evidence for liquid-liquid separation in supersaturated CaCO3 solutions. *Science* **2013**, *341*, 885.
[12] J. Baumgartner, A. Dey, P. H. H. Bomans, C. Le Coadou, P. Fratzl, M. N. A. J. Sommerdijk, D. Faivre, Nucleation and growth of magnetite from solution. *Nat. Mater.* **2013**, *12*, 310.
[13] P. J. M. Smeets, K. R. Cho, R. G. E. Kempen, M. N. A. J. Sommerdijk, J. J. De Yoreo, Calcium carbonate nucleation driven by ion binding in a biomimetic matrix revealed by in situ electron microscopy. *Nat. Mater.* **2015**, *14*, 394.
[14] N. Pienack, W. Bensch, In-situ monitoring of the formation of crystalline solids. *Angew. Chem. Int. Ed. Engl.* **2011**, *50*, 2014.
[15] A. Sarfraz, M. C. Schlegel, J. Wright, F. Emmerling, Advanced gas hydrate studies at ambient conditions using suspended droplets. *Chem. Commun.* **2011**, *47*, 9369.
[16] M. C. Schlegel, A. Sarfraz, U. Muller, U. Panne, F. Emmerling, First seconds in a building's lifeuin situ synchrotron x-ray diffraction study of cement hydration on the millisecond timescale. *Angew. Chem. Int. Ed. Engl.* **2012**, *51*, 4993.
[17] F. Delissen, J. Leiterer, R. Bienert, F. Emmerling, A. F. Thunemann, Agglomeration of proteins in acoustically levitated droplets. *Anal. Bioanal. Chem.* **2008**, *392*, 161.
[18] J. Leiterer, F. Delissen, F. Emmerling, A. F. Thunemann, U. Panne, Structure analysis using acoustically levitated droplets. *Anal. Bioanal. Chem.* **2008**, *391*, 1221.
[19] J. Leiterer, F. Emmerling, U. Panne, W. Christen, K. Rademann, Tracing coffee tabletop traces. *Langmuir* **2008**, *24*, 7970.
[20] S. E. Wolf, J. Leiterer, M. Kappl, F. Emmerling, W. Tremel, Early homogenous amorphous precursor stages of calcium carbonate and subsequent crystal growth in levitated droplets. *J. Am. Chem. Soc.* **2008**, *130*, 12342.
[21] J. Leiterer, F. Emmerling, J. Radnik, U. Bentrup, A. Bruckner, Flying droplets as model system for spray drying-An in situ synchrotron X-ray scattering study on complex oxides catalyst precursors. *Catal. Today* **2010**, *155*, 326.
[22] J. Radnik, U. Bentrup, J. Leiterer, A. Bruckner, F. Emmerling, Levitated droplets as model system for spray drying of complex oxides: a simultaneous in situ x-ray diffraction/raman study. *Chem. Mater.* **2011**, *23*, 5425.
[23] L. Trobs, Y. N. Thi, D. Rump, F. Emmerling, Crystallization behavior of carbamazepine. *Z. Phys. Chem.* **2014**, *228*, 493.
[24] J. Stroh, M. C. Schlegel, W. Schmidt, Y. N. Thi, B. Meng, F. Emmerling, Time-resolved in situ investigation of Portland cement hydration influenced by chemical admixtures. *Constr. Build. Mater.* **2016**, *106*, 18.
[25] Y. N. Thi, K. Rademann, F. Emmerling, Direct evidence of polyamorphism in paracetamol. *Crystengcomm* **2015**, *17*, 9029.
[26] T. Gnutzmann, Y. N. Thi, K. Rademann, F. Emmerling, Solvent-triggered crystallization of polymorphs studied in situ. *Cryst. Growth Des.* **2014**, *14*, 6445.
[27] M. C. Schlegel, K. J. Wenzel, A. Sarfraz, U. Panne, F. Emmerling, A wall-free climate unit for acoustic levitators. *Rev. Sci. Instrum.* **2012**, *83*, article no: 055101.
[28] K. Nagashio, Y. Takamura, K. Kuribayashi, Containerless solidification of peritectic and eutectic ceramics using aero-acoustic levitator. *Mater. Sci. Forum.* **2000**, *329–3*, 173.
[29] Y. Cerenius, A. Oskarsson, S. Santesson, S. Nilsson, L. Kloo, Preliminary tests on the use of an acoustic levitator for liquid X-ray diffraction experiments. *J. Appl. Crystallogr.* **2003**, *36*, 163.
[30] J. Leiterer, W. Leitenberger, F. Emmerling, A. F. Thunemann, U. Panne, The use of an acoustic levitator to follow crystallization in small droplets by energy-dispersive X-ray diffraction. *J. Appl. Crystallogr.* **2006**, *39*, 771.
[31] S. E. Wolf, L. Mueller, R. Barrea, C. J. Kampf, J. Leiterer, U. Panne, T. Hoffmann, F. Emmerling, W. Tremel, Carbonate-coordinated metal complexes precede the formation of liquid amorphous mineral emulsions of divalent metal carbonates. *Nanoscale* **2011**, *3*, 1158.
[32] S. E. Wolf, J. Leiterer, V. Pipich, R. Barrea, F. Emmerling, W. Tremel, Strong stabilization of amorphous calcium carbonate emulsion by ovalbumin: gaining insight into the mechanism of 'polymer-induced liquid precursor' processes. *J. Am. Chem. Soc.* **2011**, *133*, 12642.
[33] O. Paris, C. H. Li, S. Siegel, G. Weseloh, F. Emmerling, H. Riesemeier, A. Erko, P. Fratzl, A new experimental station for simultaneous X-ray microbeam scanning for small- and wide-angle scattering and fluorescence at BESSY II. *J. Appl. Crystallogr.* **2007**, *40*, S466.
[34] A. P. Hammersley, S. O. Svensson, M. Hanfland, A. N. Fitch, D. Hausermann, Two-dimensional detector software: from real detector to idealised image or two-theta scan. *High Pressure Res.* **1996**, *14*, 235.
[35] G. A. Stephenson, T. B. Borchardt, S. R. Byrn, J. Bowyer, C. A. Bunnell, S. V. Snorek, L. Yu, Conformational and color polymorphism of 5-methyl-2- (2-nitrophenyl)amino-3-thiophenecarbonitrile. *J. Pharm. Sci.* **1995**, *84*, 1385.
[36] S. Chen, I. A. Guzei, L. Yu, New polymorphs of ROY and new record for coexisting polymorphs of solved structures. *J. Am. Chem. Soc.* **2005**, *127*, 9881.
[37] C. A. Mitchell, L. Yu, M. D. Ward, Selective nucleation and discovery of organic polymorphs through epitaxy with single crystal substrates. *J. Am. Chem. Soc.* **2001**, *123*, 10830.
[38] A. M. Triggle, E. Shefter, D. J. Triggle, Crystal-structures of calcium channel antagonists – 2,6-dimethyl-3,5-dicarbomethoxy-4-[2-nitro, 3-cyano, 4-(dimethylamino), and 2,3,4,5,6-pentafluorophenyl]-1,4-dihydropyridine. *J. Med. Chem.* **1980**, *23*, 1442.
[39] E. Gunn, I. A. Guzei, T. Cai, L. Yu, Polymorphism of nifedipine: crystal structure and reversible transition of the metastable beta polymorph. *Cryst. Growth Des.* **2012**, *12*, 2037.
[40] M. Bortolotti, I. Lonardelli, G. Pepponi, Determination of the crystal structure of nifedipine form C by synchrotron powder diffraction. *Acta Crystallogr. B* **2011**, *67*, 357.
[41] M. Haisa, S. Kashino, R. Kawai, H. Maeda, Monoclinic form of para-hydroxyacetanilide. *Acta Crystallogr. B* **1976**, *32*, 1283.
[42] M. Haisa, S. Kashino, H. Maeda, Orthorhombic form of para-hydroxyacetanilide. *Acta Crystallogr. B* **1974**, *30*, 2510.
[43] M. A. Perrin, M. A. Neumann, H. Elmaleh, L. Zaske, Crystal structure determination of the elusive paracetamol Form III. *Chem. Commun.* **2009**, 3181.
[44] L. Yu, Color changes caused by conformational polymorphism: optical-crystallography, single-crystal spectroscopy, and computational chemistry. *J. Phys. Chem. A* **2002**, *106*, 544.
[45] M. Klimakow, J. Leiterer, J. Kneipp, E. Rossler, U. Panne, K. Rademann, F. Emmerling, Combined synchrotron XRD/Raman measurements: in situ identification of polymorphic transitions during crystallization processes. *Langmuir* **2010**, *26*, 11233.
[46] W. Ostwald, Studien über die Bildung und Umwandlung fester Körper. *Z. Phys. Chem.* **1897**, *22*, 289.

[47] T. Threlfall, Structural and thermodynamic explanations of Ostwald's rule. *Org. Process Res. Dev.* **2003**, *7*, 1017.
[48] B. C. Hancock, E. Y. Shalaev, S. L. Shamblin, Polyamorphism: a pharmaceutical science perspective. *J. Pharm. Pharmacol.* **2002**, *54*, 1151.
[49] R. J. Hemley, J. Badro, D. M. Teter. Polymorphism in crystalline and amorphous silica at high pressures. In *Physics Meets Mineralogy,* (Eds. H. Aoki, Y. Syono and R. J. Hemley) Cambridge University Press, Cambridge, UK, pp. 173–204, **2000**.
[50] J. H. E. Cartwright, A. G. Checa, J. D. Gale, D. Gebauer, C. I. Sainz-Diaz, Calcium carbonate polyamorphism and its role in biomineralization: how many amorphous calcium carbonates are there? *Angew. Chem. Int. Edit.* **2012**, *51*, 11960.